CHAPTER 8

Virtual Screening of Phytochemicals in Search of a Potential Drug Candidate for COVID-19: DFT Study and Molecular Docking

Nikita Tiwari[1,*], **Lubna Jamal**[1] and **Anil Mishra**[1]

[1] *Department of Chemistry, University of Lucknow, Lucknow-226007, Uttar Pradesh, India*

Abstract: The global health pandemic due to COVID-19 caused by SARS-CoV-2, affected and changed the world's condition drastically. Herein, we evaluated the bioactivity of some phytochemicals as inhibitors against SARS-CoV-2 M provirus (6LU7) using computational models. We reported the optimization of phytochemicals employing density functional theory (DFT) with B3LYP/6-311G+(d,p) level theory. DFT calculations were employed to determine the free energy, dipole moment as well as chemical reactivity descriptors. Molecular docking has been performed against the SARS-CoV-2 M provirus to search the binding affinity and interactions of all compounds with the respective protein. The known drug, Chloroquine of SARS-CoV-2 main protease, was also docked to evaluate its binding affinity. Besides, the data from DFT, the docking studies predicted that flavonoids (Quercetin, Myricetin, Apigenin and Daidzein) have the least binding affinity and might serve as a potent inhibitor against SARS-CoV-2 comparable with the approved medicine, Chloroquine. The high binding affinity of flavonoids was attributed to the presence of hydrogen bonds along with different hydrophobic interactions between the flavonoid and the critical amino acid residues of the receptor. The DFT calculations showed that flavonoids have high-lying HOMO, electrophilicity index and dipole moment. All these parameters could share a different extent to significantly affect the binding affinity of these phytochemicals with active protein sites.

Keywords: Apigenin, B3LYP, Chloroquine, COVID-19, DFT Calculations, Daidzein, Dipole Moment, Electrophilicity Index, Flavonoids, HOMO, Hydrogen Bonds, Hydrophobic Interactions, Molecular Docking, Myricetin, Pandemic, Phytochemicals, Quercetin, SARS-CoV-2.

INTRODUCTION

In the final month of the year 2019, a major cluster of strange pneumonia due to a novel coronavirus was reported in Wuhan metropolis, China [1]. Despite efforts to

---

[*] **Corresponding author Nikita Tiwari:** Department of chemistry, Lucknow University, Lucknow-226007, Uttar Pradesh, India: E-mail: nikitalko23@gmail.com

include the outbreak inside the preliminary place, the dissemination of SARS-CoV-2 has continued to spread widely to different countries. Therefore, in March 2020, the WHO declared the uncontrollable spread of SARS- CoV-2 as a pandemic [2]. Now, after more than two years after the initiation of the infection, this disease is still a threat to human life [3]. The control of SARS- CoV-2 is the need of the hour not only for human health but also for the prosperity of the nations and the betterment of society, and to achieve this purpose, global collaborations are very important [4].

Coronavirus (CoV), the virus responsible for COVID-19, belongs to the family Coronaviridae. They have spikes on their surfaces and contribute to a huge group of viruses containing RNA genome [5]. Based on the genetic and serological relationship, the coronaviruses are broadly classified into four major groups- Alpha, Beta, Gamma and Delta [6]. These RNA viruses are mainly distributed among birds and mammals [7] and have a very high potential to infect the human respiratory system [7, 8]. HCoV-OC43, -229E, -NL63, -HKU1, SARS-CoV (Severe Acute Respiratory Syndrome – Coronavirus), MERS-CoV (Middle East Respiratory Syndrome – Coronavirus) and now SARS-CoV-2 are a few examples of coronaviruses that infect humans [6, 9].

In the search for the cure, complete knowledge of the cause is pretty much important. Cryogenic electron microscopic studies and many other studies show that SARS-CoV-2 binds to the cell membrane of ACE2 (Angiotensin-converting enzyme 2) [10, 11]. The genome of coronavirus carries two replicase polyproteins that undergo proteolytic processing into a set of mature NSP (non-structural proteins) that function during viral replication, including RdRp, 3CL-Mpro, Papain-like proteinase (PL2pro) and a superfamily 1-like helicase (HEL1) [12]. According to the structure, the genome of SARS-CoV-2 (novel coronavirus) encodes many important proteins for its replication in the host genome, such as M (membrane protein), S(spike protein), N (nucleocapsid protein), E (envelop protein) and coronavirus main protease. These proteins play a pivotal role in gene expression and cleave polyproteins into replication-related proteins [13, 14]. The structure of 3CL-Mpro comprises three domains, *i.e.*, I, II and III, where domains I and II are N-terminal domains while domain III is a C-terminal domain [15].

To control and cure the SARS-CoV-2 infection, drug designing and development of the vaccine are necessary. Nowadays, many researchers around the globe are involved in studying chemicals with anti-viral properties. Many naturally occurring phytochemicals have anti-viral effects and pharmacological properties [16]. According to the ancient Indian texts 'SUSHRUT SAMHITA' and 'CHARAK SAMHITA' ancient people used the different parts of plants to cure themselves of various infectious diseases [17, 18]. *Toona sinensis* [18, 19],

Jatropha curcas [18, 20], *Glycyrrhiza glabra* [18, 21], *Daucas carota* [18, 22], *Piper chaba* [18, 23], *Cinnamomum zeylanicum* [18, 24], *Zingiber officinale* [18, 25], *etc*. are some common plants that are used to treat the diseases since ancient times, or we can say that their therapeutic uses are well known. Different parts of these plants contain a large number of phytochemicals (Table **1**), and the medicinal properties of these phytochemicals provide them with a very special place in the field of drug design or medicinal research. So we can say that phytochemicals may provide potential solutions to the SARS-CoV-2 pandemic.

The inhibition property of phytochemicals is related to their ability to inhibit the virus from attaching to the 3CL-Mpro [29, 30]. In this work, we studied certain phytochemicals (*apigenin, benzoic acid, daidzein, furfural, furfuryl formate, gallic acid, 4- hydroxybenzoic acid, maltol, oxalic acid, pyragallol, salicylic acid, succinic acid, 2,3-butanediol, propionic acid, eugenol, cinnamaldehyde, caffeic acid, pentanol, piperonal, 2,3,5-trymethyl pyrazine, asparagine, quercetin, mercytin)* to understand their utility in drug designing and effectiveness against SARS-CoV-2 *via* DFT calculations and molecular docking. Molecular docking is a robust, effective, low-cost and less time-consuming process than traditional drug discovery methods [31]. *Chloroquine* is taken as a reference compound for this study.

Table 1. Plants and their constituent chemicals active against virus diseases.

Plants	Plant Image	Family	Part Used	Chemicals
Jatropha curcas	[26]	Euphorbiaceae	Leaves, Latex	Apigenin, benzoic acid, daidzein, pyragallol, salicylic acid, gallic acid
Glycyrrhiza glabra	[27]	Leguminosae	Root	Pentanol, furfural, Furfuryl formate, maltol, butanediol, propionic acid

(Table 1) cont.....

Plants	Plant Image	Family	Part Used	Chemicals
Daucas Carota	-	Apiaceae	Root	Caffeic acid, flavonoids
Piper Chaba	[23]	Piperaceae	Leaves, Stem bark	Piperanol
Cinnamomum zeylanicum	[24]	Lauraceae	Bark, Leaves, whole plant	Cinnamaldehyde, Eugenol
Zingiber officinale	-	Zingiberaceae	Rhizome, Root	Oxalic acid
Toona sinensis	[28]	Meliaceae	Leaves	Gallic acid, Quercitin

MATERIALS AND METHODS

DFT Calculations

In this study, computational calculations were done using the DFT level of theory with the hybrid functional B3LYP using 6-311G+(d, p) basis set in the gas phase in the Gaussian09 programme package [32]. The study starts with the optimization of the geometry of all the phytochemicals, and then the optimized geometrical parameters are used in the calculation of the energy of HOMO (Highest Occupied Molecular Orbital), LUMO (Lowest Unoccupied Molecular Orbital), energy gap (ΔE), dipole moment (μ) and free energy. The initial

geometry of phytochemicals was taken from an online chemical information resource named PubChem and further modified in Gaussian 09 software using GaussView5 [33]. The absence of imaginary frequency confirmed that phytochemicals were fully optimized. Chemical reactivity descriptors such as hardness (η), softness (δ), electronegativity (χ) and electrophilicity index (ω) of all the phytochemicals were also calculated from the energies of frontier HOMOs and LUMOs. The equations used for the calculations of reactivity descriptors have been reported in our earlier publications [34, 35].

Molecular Docking

The three-dimensional crystal structure of the SARS-CoV-2 M provirus (PDB ID: 6LU7) was retrieved in PDB format from an online protein data bank (PDB) [36]. All the present hetero atoms along with water molecules, were removed, and the energy minimization of the protein was implemented by Auto dock 4.2 software [37]. Then optimized phytochemicals were subjected to a molecular docking study against SARS-CoV-2 M provirus (6LU7). In computer-aided drug design, binding affinity and mode(s) of the ligand with the target protein can predict by molecular docking simulation. Finally, molecular docking simulation was performed by Auto dock Tools considering the protein as a macromolecule and the phytochemical as a ligand. In this study, rigid docking was performed where all rotatable bonds were converted into non-rotatable ones with the centre grid box size -26.346, 12.605, and 58.919 Å along x, y and z directions, respectively. The number of points in the x, y and z directions are 126, 126 and 126, respectively. After docking, both the protein and ligand structures were saved in. pdbqt format required to analyze and visualize the docking result and search the interactions between ligands and amino acid residues of the receptor protein. The results were shown using Ligplot.

RESULT AND DISCUSSION

DFT Calculation Studies

The DFT calculations were undertaken using Gaussian09 software at B3LYP 6-311G+(d,p) basis set. The optimized structures (Fig. **1**) of the phytochemicals were drawn with Gauss View 5.

Thermodynamic Properties

The thermodynamic properties, such as free energy, are important to predict the stability of any given chemical reaction. Greater negative values indicate improved thermodynamic properties. This study found that the values are negative (Table **2**), meaning the binding will occur spontaneously without any extra energy

expenditure. The free energy of Chloroquine is -1326.289 Hartree, whereas flavonoids show similar energy, which suggests that the molecules are energetically and configurationally more preferable. The dipole moment of Chloroquine is 7.113 Debye, where flavonoids show a near about dipole moment to the chloroquine. The elevated level of dipole moment enhances the hydrogen bond formation, nonbonding interaction, binding affinity and polar nature of a molecule.
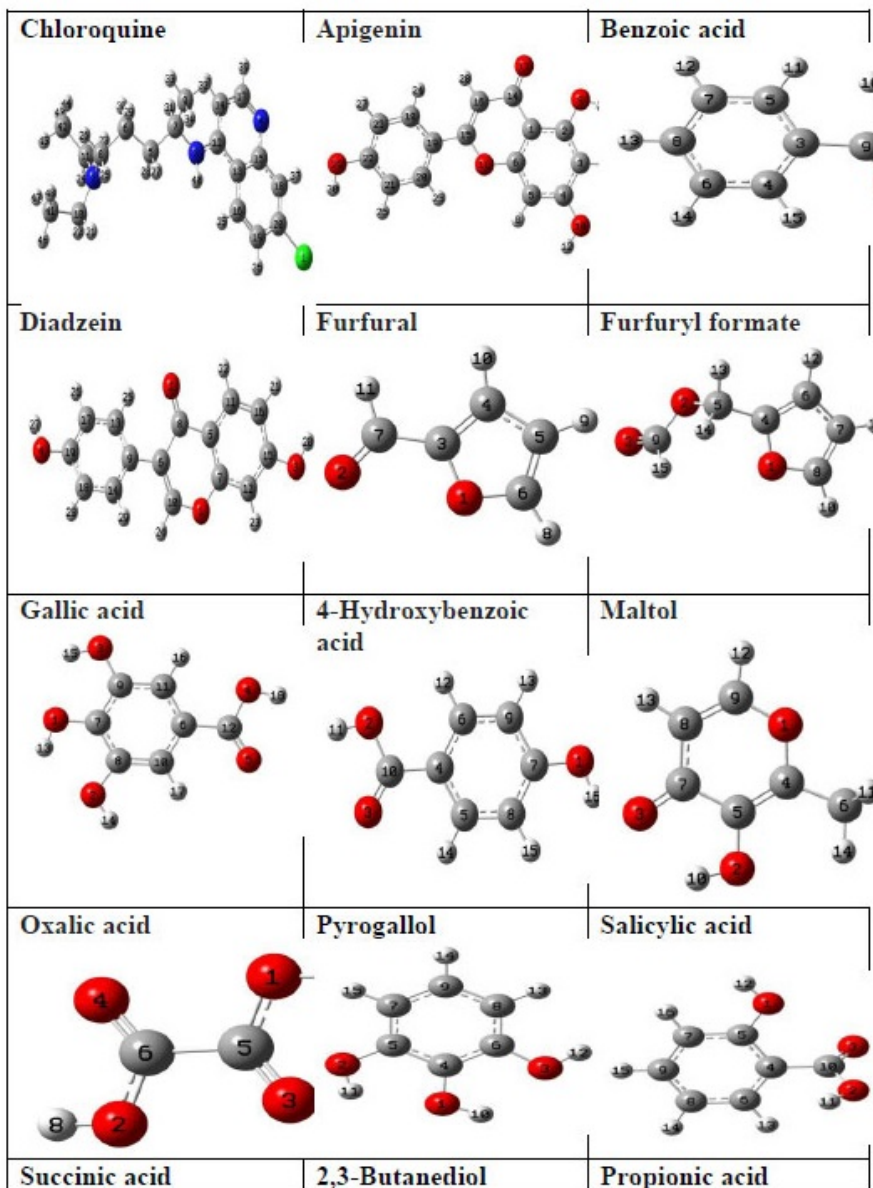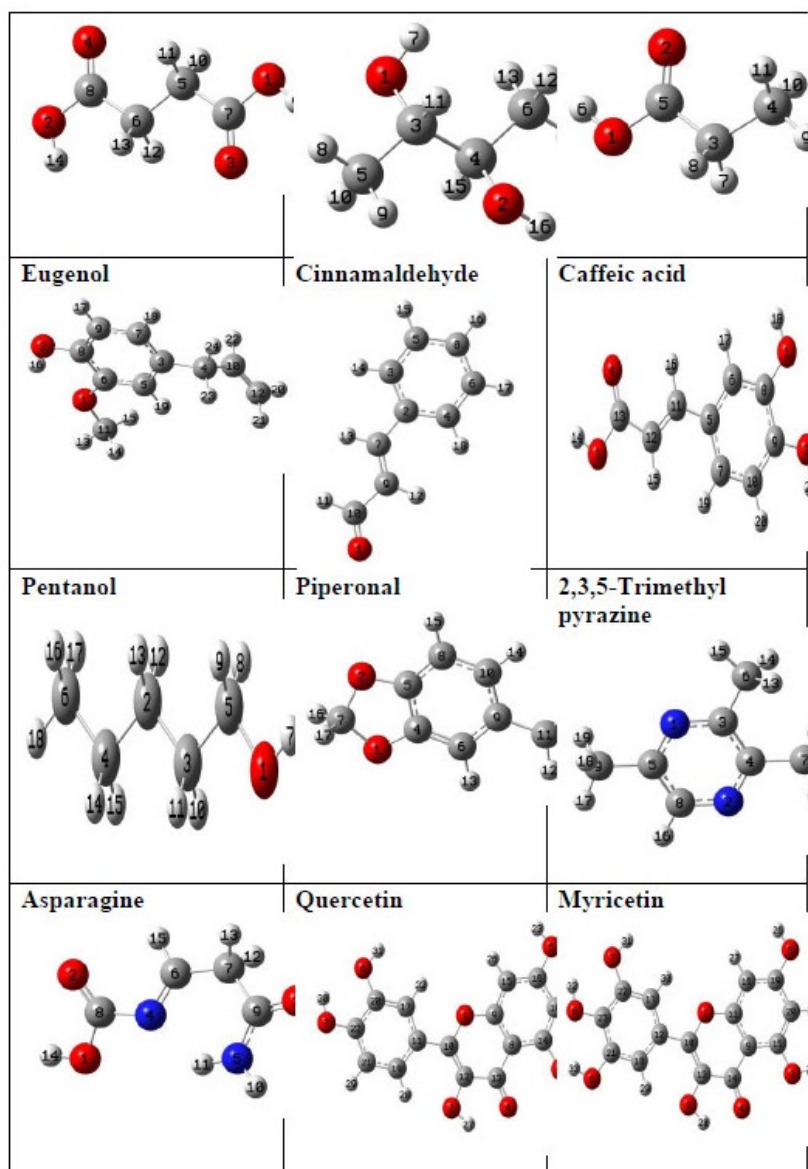
Fig. (1). The optimized structure of investigated phytochemicals and chloroquine.

Table 2. Free energy (in Hartree) and dipole moment (Debye) of chloroquine and all the phytochemicals.

Ligand	Free Energy	Dipole Moment
Chloroquine	-1326.289	7.113
Apigenin	-953.994	6.586

(Table 2) cont.....

Ligand	Free Energy	Dipole Moment
Benzoic acid	-420.937	5.050
Diadzein	-878.748	2.332
Furfural	-343.446	4.521
Furfuryl formate	-458.020	4.845
Gallic acid	-646.694	2.344
4-Hydroxybenzoic acid	-496.197	1.926
Maltol	-458.039	3.702
Oxalic acid	-378.448	0.051
Pyrogallol	-458.055	2.973
Salicylic acid	-496.178	5.784
Succinic acid	-457.112	3.002
2,3-Butanediol	-308.989	2.275
Propionic acid	-268.489	1.612
Eugenol	-538.856	2.643
Cinnamaldehyde	-423.092	4.917
Caffeic acid	-648.861	2.413
Pentanol	-273.067	1.623
Piperonal	-534.133	4.314
2,3,5-Trimethyl pyrazine	-382.381	0.649
Asparagine	-491.388	3.127
Quercetin	-1104.495	6.493
Myricetin	-1179.742	7.283

Molecular Orbital Properties

The hardness and softness of a molecule can be obtained from its energy gap, *i.e.*, the HOMO-LUMO gap. The large energy gap is related to high kinetic stability and low chemical reactivity, and the small energy gap represents low chemical stability because the addition of electrons to a higher LUMO and the withdrawal of electrons from a lower HOMO is energetically favourable in a certain reaction. In this analysis, Chloroquine has a HOMO-LUMO gap of 4.30 eV (Fig. **2**), where flavonoids Quercetin (3.74 eV) and Myricetin (3.77 eV) shows the lower energy gap and the lower chemical potential (-3.89 eV) with the highest chemical softness (0.53 eV) values as compared to the chloroquine which may contribute the higher chemical reactivity than others (Table **3**).
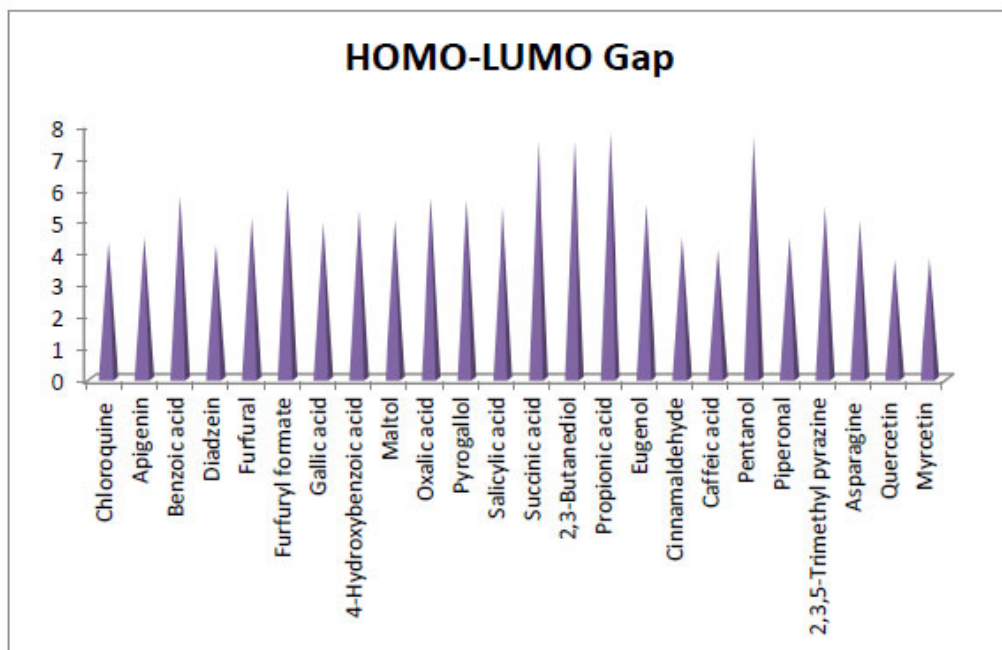
Fig. (2). Pictorial representation of energy gap (HOMO-LUMO gap) for all the investigated compounds.

Table 3. HOMO, LUMO, gap, hardness (η), softness (δ), electronegativity (χ), electrophilicity index (ω), ionization potential (I) and electron affinity (A) of all the compounds.

Ligand	HOMO	LUMO	ΔE	χ	η	δ	ω	I	A
Chloroquine	-5.81	-1.51	4.30	-3.66	2.15	0.46	3.11	5.81	1.51
Apigenin	-6.30	-1.85	4.45	-4.07	2.22	0.45	3.73	6.30	1.85
Benzoic acid	-7.63	-1.88	5.75	-4.75	2.87	0.34	3.93	7.63	1.88
Diadzein	-6.06	-1.85	4.21	-3.95	2.10	0.47	3.71	6.06	1.85
Furfural	-7.20	-2.15	5.05	-4.67	2.52	0.39	4.32	7.20	2.15
Furfuryl formate	-6.91	-0.92	5.99	-3.91	2.99	0.33	2.55	6.91	0.92
Gallic acid	-6.51	-1.61	4.90	-4.06	2.45	0.40	3.36	6.51	1.61
4-Hydroxybenzoic acid	-6.85	-1.57	5.28	-4.21	2.64	0.37	3.35	6.85	1.57
Maltol	-6.64	-1.66	4.98	-4.15	2.49	0.40	3.45	6.64	1.66
Oxalic acid	-8.16	-2.49	5.67	-5.32	2.83	0.35	5.00	8.16	2.49
Pyrogallol	-6.12	-0.51	5.61	-3.31	2.80	0.35	1.95	6.12	0.51
Salicylic acid	-6.92	-1.53	5.39	-4.22	2.69	0.37	3.31	6.92	1.53
Succinic acid	-8.07	-0.63	7.44	-4.35	3.72	0.26	2.54	8.07	0.63
2,3-Butanediol	-7.66	-0.18	7.48	-3.92	3.74	0.26	2.05	7.66	0.18

(Table 3) cont.....

Ligand	HOMO	LUMO	ΔE	χ	η	δ	ω	I	A
Propionic acid	-7.96	-0.23	7.73	-4.09	3.86	0.25	2.16	7.96	0.23
Eugenol	-5.86	-0.39	5.47	-3.12	2.73	0.36	1.78	5.86	0.39
Cinnamaldehyde	-6.95	-2.51	4.44	-4.73	2.22	0.45	5.03	6.95	2.51
Caffeic acid	-6.20	-2.16	4.04	-4.18	2.02	0.49	4.32	6.20	2.16
Pentanol	-7.60	-0.01	7.59	-3.80	3.79	0.26	1.90	7.60	0.01
Piperonal	-6.42	-1.98	4.44	-4.20	2.22	0.45	3.97	6.42	1.98
2,3,5-Trimethyl pyrazine	-6.78	-1.39	5.39	-4.08	2.69	0.37	3.09	6.78	1.39
Asparagine	-7.35	-2.39	4.96	-4.87	2.48	0.40	4.78	7.35	2.39
Quercetin	-5.76	-2.02	3.74	-3.89	1.87	0.53	4.04	5.76	2.02
Myricetin	-5.78	-2.01	3.77	-3.89	1.88	0.53	4.02	5.78	2.01

Binding Affinity and Binding Interactions Analysis

Docking simulation studies were done to predict the binding mode of phytochemicals at the SARS-CoV-2 M pro pocket (Fig. **3**). Similarly, the Chloroquine was docked in the protein pocket as a control. The binding affinity of phytochemicals ranged between -1.22 to -6.36 Kcal/mol. The results showed that flavonoids are located in the active pocket, similar to chloroquine. Chloroquine showed binding energy of -4.79 kcal/mol (Fig. **4**), whereas increasing order of binding energy followed the sequence such as Myricetin<Quercetin<Apigenin<Daidzein (-5.49<-5.68<-5.8<-6.36) kcal/mol. Except for ordinary hydrogen bonding, nonbonding interactions have frequently used the term to determine the shape and behaviour of molecules. From molecular docking analysis, the major and common residues of 6LU7 active sites like HIS163, CYS145, MET165, THR190, HIS164, LEU167, GLU166, GLN189 and PRO168 form different significant interactions with the ligands (Table **4**).

Table 4. Binding affinity and non-binding interactions of all the investigated compounds.

Ligand	Binding Energy	Interacting Amino Acids
Chloroquine	-4.79	HIS163, CYS145, MET165, THR190, HIS164, LEU167, GLU166, GLN189, PRO168
Apigenin	-5.8	HIS163, CYS145, GLU166, GLN189, MET165, ASP187, ARG188, HIS41, HIS164, LEU141 (2.92 Å), SER144 (2.84 Å)
Benzoic acid	-3.76	ARG4, PHE291, LEU282, TRP207, PHE3, GLU288, LYS5 (3.16 Å)
Daidzein	-6.36	GLU166, MET165, ASP187, ARG188, MET49, GLN189, HIS164, HIS163, LEU141, CYS145 (3.04 Å), PHE140 (3.07 Å)

(Table 4) cont.....

Ligand	Binding Energy	Interacting Amino Acids
Furfural	-3.28	HIS164, MET165, ARG188, TYR54, GLN189, MET49, HIS41, PRO52, ASP187
Furfuryl formate	-2.95	PRO52, MET49, ARG188, MET165, GLN189, HIS41, ASP187, TYR54 (2.92 Å)
Gallic acid	-2.74	PHE219, GLU270, LEU271, TRP218, ASN221 (3.26 Å), ARG279 (2.71 Å), GLY275 (2.87 Å)
4-Hydroxybenzoic acid	-3.77	ARG4, GLU288, PHE291, LEU282, PHE3, LYS5 (3.13 Å), TRP207 (2.72 Å)
Maltol	-3.32	LEU75, VAL77, ARG76, GLN74, PHE66, LEU67, HIS64 (2.63 Å)
Oxalic acid	-1.64	VAL303, GLY302 (3.05 Å), SER1 (2.85 Å & 3.19 Å)
Pyrogallol	-3.04	ASN63, HIS64, ARG76, LEU67, GLN74 (3.26 Å), PHE66 (2.94 Å & 2.99 Å), VAL77 (2.77 Å & 3.03 Å)
Salicylic acid	-3.6	LYS5, ARG4, PHE291, LEU282, SER284, GLU288, TRP207, PHE3 (3.03 Å)
Succinic acid	-1.22	HIS80, LYS90, GLY79, VAL35, LYS88, SER81
2,3-Butanediol	-2.27	PHE3, TRP207, SER284, GLU288, LEU282 (2.89 Å & 3.05 Å)
Propionic acid	-1.96	MET17, GLY15, GLU14 (3.02 Å), LYS97 (2.74 Å)
Eugenol	-4.36	MET165, TYR54, ASP187, MET49, GLN189, THR190, ARG188, GLU166 (3.04 Å & 3.32 Å)
Cinnamaldehyde	-4.19	MET165, GLN189, ASP187, HIS41, ARG188, HIS164, GLU166
Caffeic acid	-3.55	GLU288, PHE291, PHE3, ARG4, LYS5, SER284, LEU282, TRP207 (2.60 Å)
Pentanol	-2.61	PRO52, ARG188, MET165, HIS164, ASP187, GLN189, MET49, HIS41, TYR54 (2.72 Å)
Piperonal	-4.18	MET165, GLN189, HIS41, MET49, ASP187, ARG188, PRO52, TYR54, HIS164
2,3,5-Trimethyl pyrazine	-4.16	MET49, ARG188, HIS41, HIS164, MET165, TYR54, ASP187, PRO52
Asparagine	-2.79	ARG4, LYS5, PHE3, PHE291, LEU282, TRP207 (2.94 Å)
Quercetin	-5.68	HIS41, GLN189, MET165, GLU166, PRO168, LEU167, THR190, ARG188, TYR54 (2.77 Å), ASP187 (3.14 Å)
Myricetin	-5.49	HIS164, MET165, GLU166, PRO168, LEU167, ARG188, GLN189, HIS41 (3.31 Å), TYR54 (2.85 Å), THR190 (2.89 Å & 3.00 Å), ASP187 (3.02 Å), GLN192 (3.06 Å)
-	-	-
-	-	-

(Table 4) cont.....

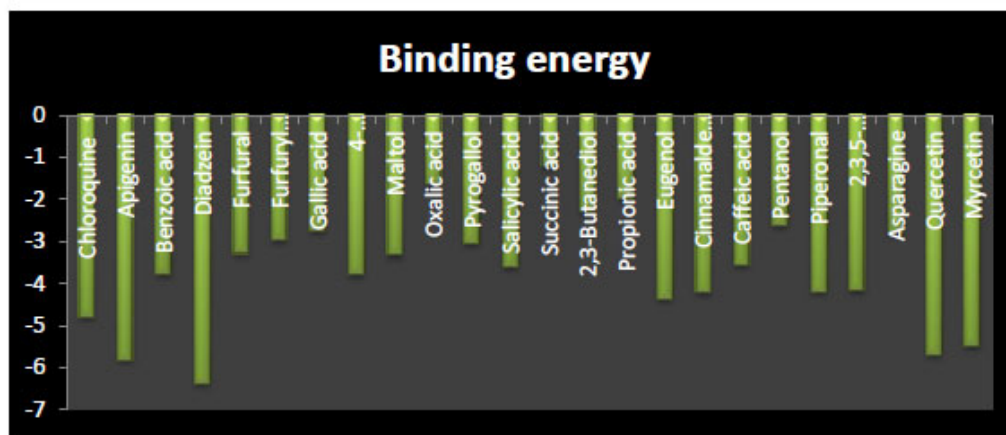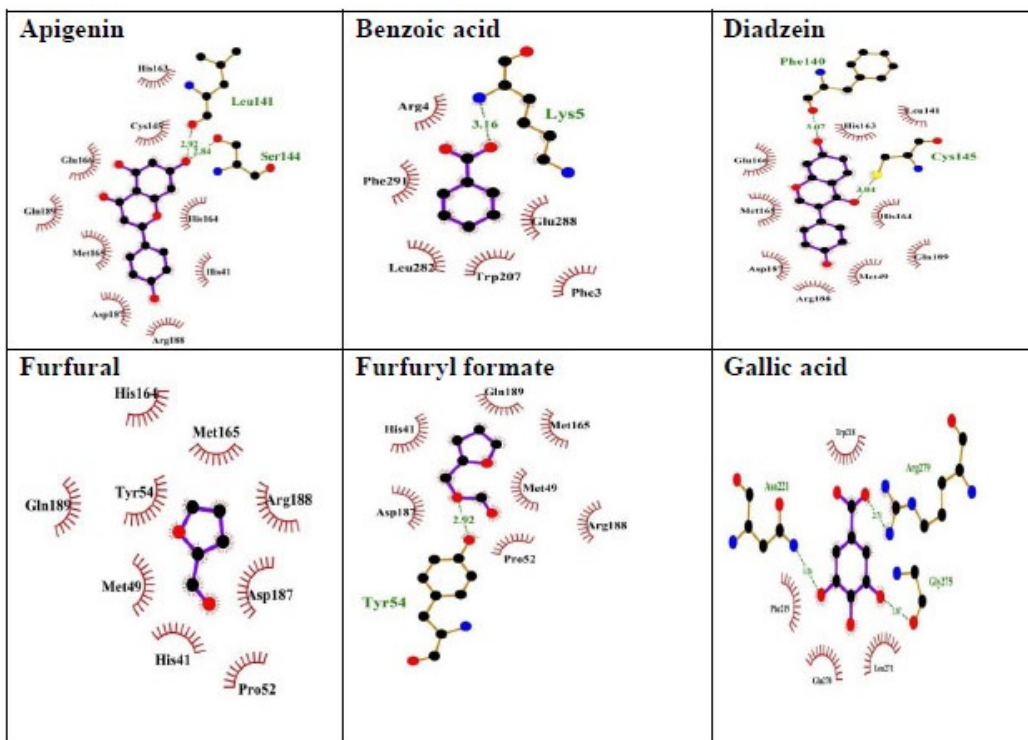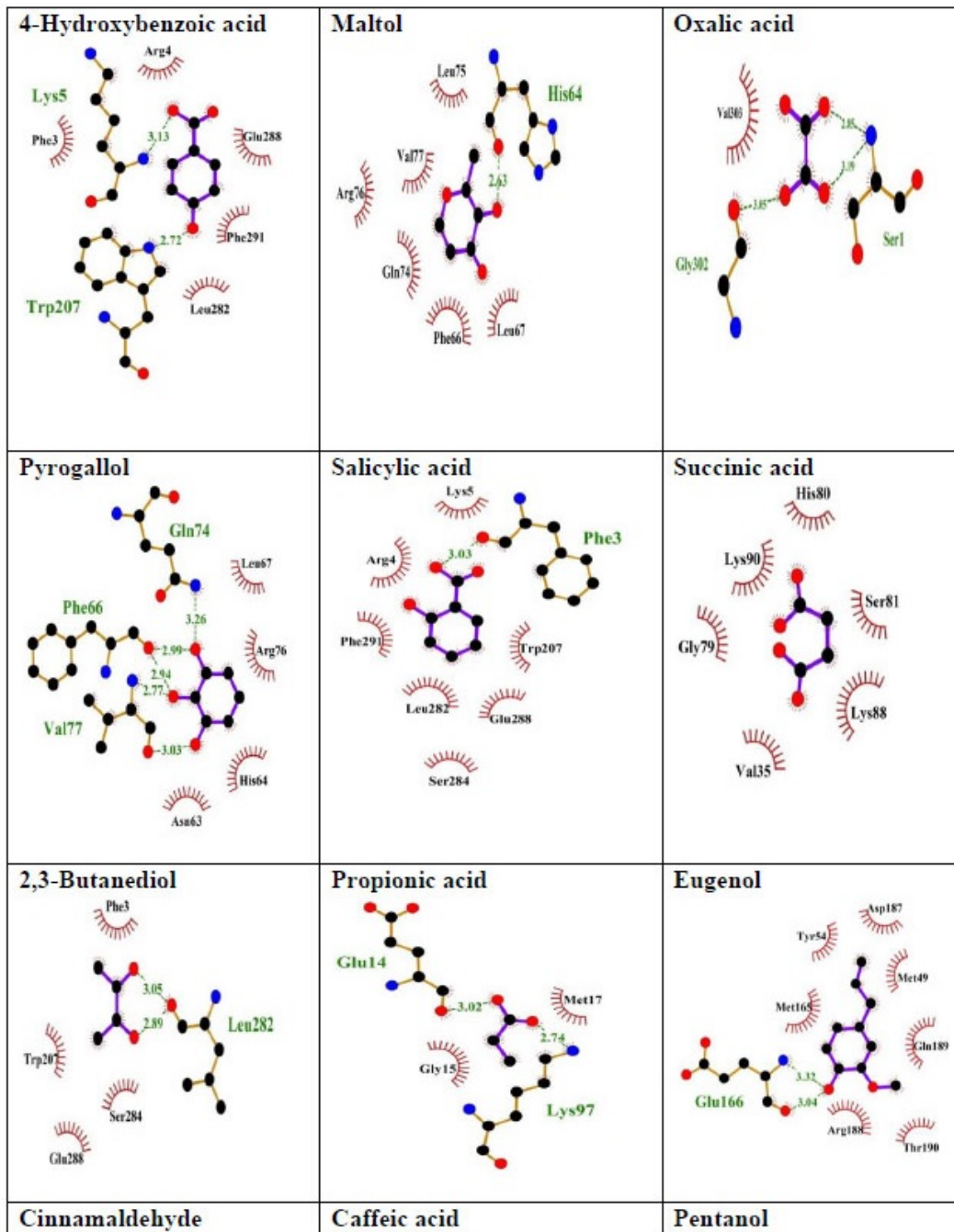| Ligand	Binding Energy	Interacting Amino Acids
-	-	-
-	-	-
-	-	-
-	-	-
-	-	-
-	-	-

Fig. (3). Graphical representation of binding energies of all the selected compounds.

AutoDock results show that among all the phytochemicals(taken in this study), the binding affinities of apigenin(-5.8 kcal/mol), daidzein(-6.36 kcal/mol), quercetin(-5.68kcal/mol) and myricetin(-5.49 kcal/mol) is comparable to well-known ligand chloroquine(-4.79 kcal). Daidzein showed the lowest binding affinity and interacted hydrophobically with the residues GLU166, MET165, ASP187, ARG188, MET49, GLN189, HIS164, HIS163 AND LEU141. The polar interactions were found to be with Phe140(3.07 Å) and CYS 145(3.04 Å). Hydrogen bonding and different hydrophobic interactions between the inhibitor and the amino acid residues of the receptor are responsible for the binding affinity of daidzein. The result of the docking studies shows that the amino acid residue HIS163, CYS145, GLU166, GLN189, MET165, ASP187, ARG188, HIS41, and HIS164 interacted hydrophobically with the apigenin molecule, whereas LEU141(2.92 Å) and SER144(2.84 Å) show polar interactions. The phytochemical quercetin also shows good interaction with 3CL-Mpro. The hydrophobic interaction was found with residues HIS41, GLN189, MET165, GLU166, PRO168, LEU167, THR190 and ARG188; and hydrogen bonding with Tyr54(2.77 Å) and Asp187(3.14 Å). However, myricetin interacts

hydrophobically with HIS164, MET165, GLU166, PRO168, LEU167, ARG188 and GLA189. Tyr54(2.85 Å), His41(3.31 Å), Asp187(3.02 Å), Gln192(3.06 Å) and Thr190(2.89 Å) show polar interactions. Hence, these phytochemicals have the potential to combat SARS-CoV-2.
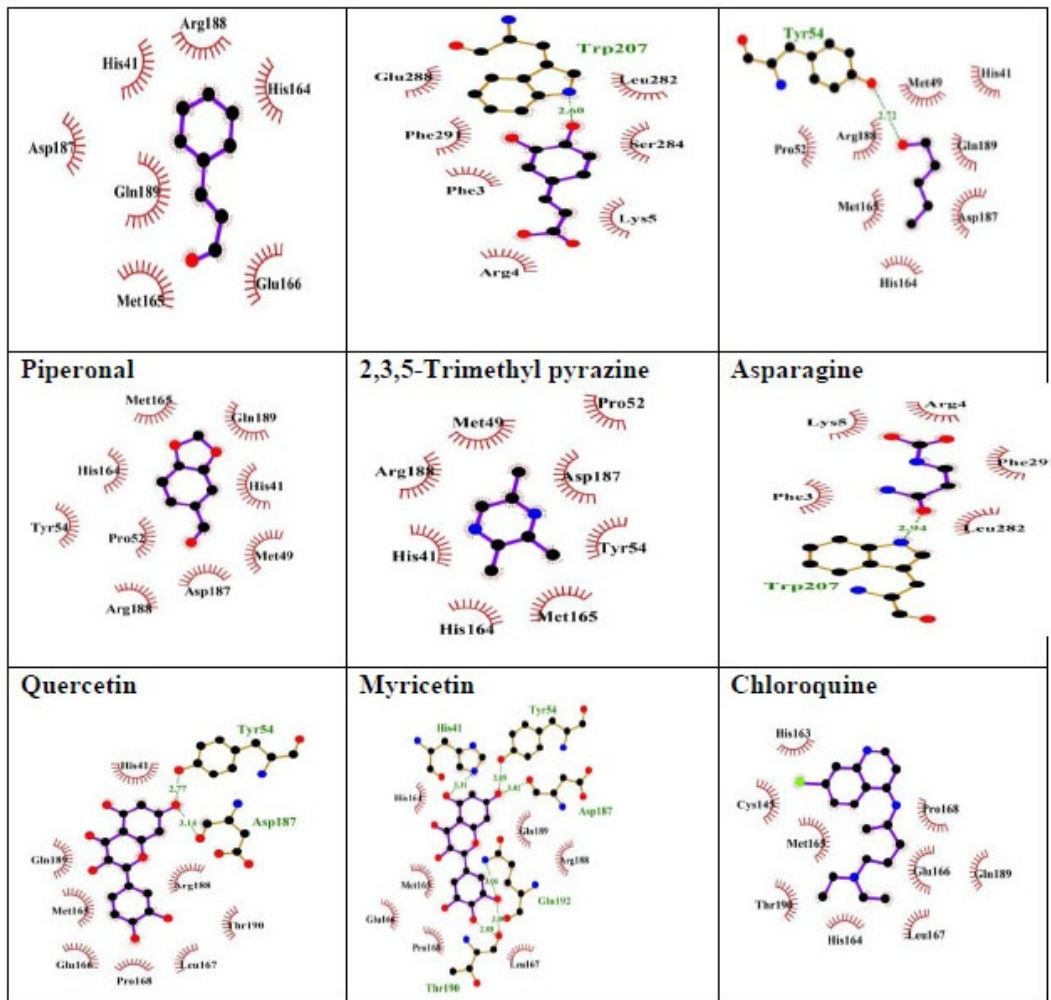
4-Hydroxybenzoic acid

Arg4
Lys5
Phe3
3.13
Glu288
Phe291
2.72
Trp207
Leu282

Maltol

Leu75
His64
Val77
2.63
Arg76
Gln74
Phe66   Leu67

Oxalic acid

Val36
2.85
Val340
1.96
3.05
Gly302
Ser1

Pyrogallol

Gln74
Leu67
Phe66
3.26
Arg76
2.99
2.94
2.77
Val77
3.03
His64
Asn63

Salicylic acid

Lys5
Phe3
Arg4
3.03
Phe291
Trp207
Leu282   Glu288
Ser284

Succinic acid

His80
Lys90
Ser81
Gly79
Lys88
Val35

2,3-Butanediol

Phe3
3.05
2.89
Leu282
Trp207
Ser284
Glu288

Propionic acid

Glu14
Met17
3.02
2.74
Gly15
Lys97

Eugenol

Asp187
Tyr54
Met49
Met165
Gln189
3.32
Glu166   3.04
Arg188
Thr190

| Cinnamaldehyde | Caffeic acid | Pentanol |

Fig. (4). Amino acid residues in the binding pocket of SARS-CoV-2 M pro involved in interactions with the phytochemicals and chloroquine.

CONCLUSION

In this study, the inhibitory action of phytochemicals against the SARS-CoV-2 M provirus has been studied. From the DFT calculations, all the compounds are thermally stable, and some (flavonoids) of them show better chemical reactivity than Chloroquine, a known drug. Among all the phytochemicals studied, Flavonoids show greater dipole moments with a smaller energy gap. The docking results also confirmed that flavonoids with lower binding affinities than chloroquine are more potent inhibitors against the SARS-CoV-2 M provirus. This

study may be helpful in understanding the physicochemical and biological properties of phytochemicals against this novel coronavirus.

CONSENT FOR PUBLICATION

Not applicable.

CONFLICT OF INTEREST

The authors declare no conflict of interest, financial or otherwise.

ACKNOWLEDGEMENTS

REFERENCES

[1]   Wang Y, Wang Y, Chen Y, Qin Q. Unique epidemiological and clinical features of the emerging 2019 novel coronavirus pneumonia (COVID-19) implicate special control measures. J Med Virol 2020; 92(6): 568-76.
[http://dx.doi.org/10.1002/jmv.25748] [PMID: 32134116]

[2]   Zhou P, Yang XL, Wang XG, *et al.* A pneumonia outbreak associated with a new coronavirus of probable bat origin. Nature 2020; 579(7798): 270-3.
[http://dx.doi.org/10.1038/s41586-020-2012-7] [PMID: 32015507]

[3]   WHO coronavirus disease (COVID-19) dashboard. Geneva: World Health Organization 2021.

[4]   Kaur SP, Gupta V. COVID-19 Vaccine: A comprehensive status report. Virus Res 2020; 288: 198114.
[http://dx.doi.org/10.1016/j.virusres.2020.198114] [PMID: 32800805]

[5]   Peele KA, Potla Durthi C, Srihansa T, *et al.* Molecular docking and dynamic simulations for antiviral compounds against SARS-CoV-2: A computational study. Informatics in Medicine Unlocked 2020; 19: 100345.
[http://dx.doi.org/10.1016/j.imu.2020.100345] [PMID: 32395606]

[6]   Corman VM, Muth D, Niemeyer D, Drosten C. Hosts and sources of endemic human coronaviruses. In: Advances in virus research.Elsevier Inc. 2018; 100: pp. 163-88.
[http://dx.doi.org/10.1016/bs.aivir.2018.01.001]

[7]   Masters PS. The molecular biology of coronaviruses. Adv Virus Res 2006; 66(06): 193-292.
[http://dx.doi.org/10.1016/S0065-3527(06)66005-3] [PMID: 16877062]

[8]   Spaan W, Cavanagh D, Horzinek MC. Coronaviruses: structure and genome expression. J Gen Virol 1988; 69(12): 2939-52.
[http://dx.doi.org/10.1099/0022-1317-69-12-2939] [PMID: 3058868]

[9]   Andersen KG, Rambaut A, Lipkin WI, Holmes EC, Garry RF. The proximal origin of SARS-CoV-2. Nat Med 2020; 26(4): 450-2.
[http://dx.doi.org/10.1038/s41591-020-0820-9] [PMID: 32284615]

[10]   Walls AC, Park YJ, Tortorici MA, *et al.* Structure, function, and antigenicity of the SARS-CoV-2 spike glycoprotein. Cell 2020; 180: 1-12.
[http://dx.doi.org/10.1016/j.cell.2020.02.058]

[11]   Yang J, Roy A, Zhang Y. Protein–ligand binding site recognition using complementary binding-specific substructure comparison and sequence profile alignment. Bioinformatics 2013; 29(20): 2588-95.
[http://dx.doi.org/10.1093/bioinformatics/btt447] [PMID: 23975762]

[12]   Cheng A, Zhang W, Xie Y, *et al.* Expression, purification, and characterization of SARS coronavirus RNA polymerase. Virology 2005; 335(2): 165-76.
[http://dx.doi.org/10.1016/j.virol.2005.02.017] [PMID: 15840516]

[13]   Graham RL, Sparks JS, Eckerle LD, Sims AC, Denison MR. SARS coronavirus replicase proteins in pathogenesis. Virus Res 2008; 133(1): 88-100.
[http://dx.doi.org/10.1016/j.virusres.2007.02.017] [PMID: 17397959]

[14]   Prasad A, Prasad M. SARS-CoV-2: the emergence of a viral pathogen causing havoc on human existence. J Genet 2020; 99(1): 37.
[http://dx.doi.org/10.1007/s12041-020-01205-x] [PMID: 32482926]

[15]   Tassakka ACMAR, Sumule O, Massi MN, *et al.* Potential bioactive compounds as SARS-CoV-2 inhibitors from extracts of the marine red alga *Halymenia durvillei* (Rhodophyta) – A computational study. Arab J Chem 2021; 14(11): 103393.
[http://dx.doi.org/10.1016/j.arabjc.2021.103393] [PMID: 34909061]

[16]   Perez RM. Antiviral activity of compounds isolated from plants. Pharm Biol 2003; 41(2): 107-57.
[http://dx.doi.org/10.1076/phbi.41.2.107.14240]

[17]   Thakur S, Asrani RK, Patil RD, Thakur M. Antimicrobial potential of medicinal plants of Himachal Pradesh against pathogenic Escherichia Coli, Salmonella Gallinarum and Salmonella Typhimurium. Vet Res (Faisalabad) 2018; 6: 67-71.

[18]   Pal S, Chowdhury T, Paria K, *et al.* Brief survey on phytochemicals to prevent COVID-19. J Indian Chem Soc 2022; 99(1): 100244.
[http://dx.doi.org/10.1016/j.jics.2021.100244]

[19]   Chojnacka K, Witek-Krowiak A, Skrzypczak D, Mikula K, Młynarz P. Phytochemicals containing biologically active polyphenols as an effective agent against Covid-19-inducing coronavirus. J Funct Foods 2020; 73: 104146.
[http://dx.doi.org/10.1016/j.jff.2020.104146] [PMID: 32834835]

[20]   Thomas R, Sah N, Sharma P. Therapeutic biology of Jatropha curcas: a mini review. Curr Pharm Biotechnol 2008; 9(4): 315-24.
[http://dx.doi.org/10.2174/138920108785161505] [PMID: 18691091]

[21]   Hasan MK, Ara I, Mondal MSA, *et al.* Phytochemistry, pharmacological activity, and potential health benefits of Glycyrrhiza glabra. Heliyon 2021; e07240-7.
[http://dx.doi.org/10.1016/j.heliyon.2021.e07240]

[22]   Al-Snafi PDAE. Nutritional and therapeutic importance of *Daucus carota*- A review. IOSR J Pharm 2017; 7(2): 72-88.
[http://dx.doi.org/10.9790/3013-0702017288]

[23]   Haque ME, Roy AC, Rani M. Review on Phytochemical and Pharmacological Investigation of *Piper chaba* Hunter. Int J Sci Eng Res 2018; 9(3): 1.

[24]   Mishra N, Srivastava R. Therapeutic and Pharmaceutical Potential of Cinnamon. Ethnopharmacological Investigation of Indian Spices 2020. In book: Ethnopharmacological Investigation of Indian Spices (pp.124-136).
[http://dx.doi.org/10.4018/978-1-7998-2524-1.ch010]

[25]   Ghosh AK, Banerjee S, Mullick HI, *et al.* Zingiber officinale: A Natural Gold. Int J Pharma Bio Sci 2011; 2(1): 1.

[26]   Abobatta W. Jatropha curcas: an overview. J Adv Agric 2019; 10: 1650-6.

[http://dx.doi.org/10.24297/jaa.v10i0.8145]

[27] Sharma V, Agrawal RC. *Glycyrrhiza glabra*- A Plant For The Future; Mintage J Pharm Med Sci 2008.

[28] Peng W, Liu Y, Hu M, *et al. Toona sinensis*: a comprehensive review on its traditional usages, phytochemisty, pharmacology and toxicology. Rev Bras Farmacogn 2019; 29(1): 111-24.
[http://dx.doi.org/10.1016/j.bjp.2018.07.009] [PMID: 32287507]

[29] Muteeb G, Alshoaibi A, Aatif M, *et al.* Screening marine algae metabolites as high – affinity inhibitors of SARS – CoV – 2 main protease (3CLpro): an *in silico* analysis to identify novel drug candidates to combat COVID – 19 pandemic. Applied. Bioorg Chem 2020; 63(1): 1.

[30] Palese LL. The structural landscape of SARS-CoV-2 main protease: hints for inhibitor search. ChemRxiv 2020.
[http://dx.doi.org/10.26434/chemrxiv.12209744.v1]

[31] Bharti R, Shukla SK. Molecules against Covid-19: An *in silico* approach for drug development. Journal of Electronic Science and Technology 2021; 19(1): 100095.
[http://dx.doi.org/10.1016/j.jnlest.2021.100095]

[32] Frisch MJ, *et al.* Gaussian 09, Revision D01. Wallingford, CT: Gaussian, Inc. 2009.

[33] Dennington R, Keith T, Millam J. GaussView, version 5. Shawnee Mission, KS, USA: Semichem Inc. 2009.

[34] Tiwari N, Kumar A, Pandey A, Mishra A. Computational investigation of dioxin-like compounds as human sex hormone-binding globulin inhibitors: DFT calculations, docking study and molecular dynamics simulations. Comput Toxicol 2022; 21: 100198.
[http://dx.doi.org/10.1016/j.comtox.2021.100198]

[35] Tiwari N, Pandey A, Kumar A, Mishra A. Computational models reveal the potential of polycyclic aromatic hydrocarbons to inhibit aromatase, an important enzyme of the steroid biosynthesis pathway. Comput Toxicol 2021; 19: 100176.
[http://dx.doi.org/10.1016/j.comtox.2021.100176]

[36] Jin Z, Du X, Xu Y, *et al.* Structure of M[pro] from SARS-CoV-2 and discovery of its inhibitors. Nature 2020; 582(7811): 289-93.
[http://dx.doi.org/10.1038/s41586-020-2223-y] [PMID: 32272481]

[37] Morris GM, Huey R, Lindstrom W, *et al.* AutoDock4 and AutoDockTools4: Automated docking with selective receptor flexibility. J Comput Chem 2009; 30(16): 2785-91.
[http://dx.doi.org/10.1002/jcc.21256] [PMID: 19399780]